Magnetically Tuned Spin Dynamics Resonance

J. Kronjäger,[1] C. Becker,[1] P. Navez,[2,3] K. Bongs,[1] and K. Sengstock[1]

[1]Institut für Laserphysik, Universität Hamburg, Luruper Chaussee 149, D-22761 Hamburg, Germany

[2]Labo Vaste-Stoffysica en Magnetisme, Katholieke Universiteit Leuven, Celestijnenlaan 200D, B-3001 Leuven, Belgium

[3]additional address: Universität Duisburg-Essen, Universitätsstrasse 5, 45117 Essen, Germany

(Received 2 June 2006; published 12 September 2006)

We present the experimental observation of a magnetically tuned resonance phenomenon in the spin mixing dynamics of ultracold atomic gases. In particular, we study the magnetic field dependence of spin conversion in $F = 2$ ^{87}Rb spinor condensates in the crossover from interaction dominated to quadratic Zeeman dominated dynamics. We discuss the observations in the framework of spin dynamics as well as matter wave four wave mixing. Furthermore, we show that the validity range of the single mode approximation for spin dynamics is significantly extended at high magnetic field.

DOI: 10.1103/PhysRevLett.97.110404 PACS numbers: 03.75.Mn, 03.75.Gg, 32.60.+i

Ultracold quantum gas spin mixtures are currently receiving rapidly growing experimental and theoretical interest. They combine the unprecedented control achieved in single component Bose-Einstein condensates (BEC) with intrinsic degrees of freedom. The spin-dependent coupling connects quantum gas physics to fundamental magnetic phenomena. Earlier work analyzed the basic magnetic properties of these spinor condensates [1–4] and demonstrated antiferromagnetic behavior in the $F = 1$ state of ^{23}Na [5] and the $F = 2$ state of ^{87}Rb [6] as well as ferromagnetic behavior in the $F = 1$ state of ^{87}Rb [6,7].

A particularly interesting feature of these clean and undisturbed systems is that they give access to quantum aspects of magnetism such as interaction-driven spin oscillations [6–12], the quantum classical transition [13], or domain formation [5,12,14]. The magnetic field dependence of the underlying spin conversion process has been analyzed in detail for $F = 1$ spinor condensates [13,15–17] and besides oscillatory behavior, a resonance phenomenon was predicted [17]. Experiments so far focused on magnetic fields above the resonance [13] and on magnetic phase controlling of the spinor dynamics , but a spin mixing resonance has not yet been observed.

In this Letter, we study for the first time magnetic field tuned spin mixing in $F = 2$ ^{87}Rb spinor condensates. In particular as a main result, we demonstrate resonant spin mixing behavior in spinor condensates. This resonance phenomenon becomes evident in the temporal population evolution shown in Fig. 1. As a surprising central effect, the mean field driven spin dynamics (population transfer from $m_F \pm 1$ to $m_F = 0$) strongly depends on the external magnetic field. In contrast to studies on the natural ground state phase of the system and early findings on spin dynamics suppression [8,9] at high magnetic field values, we now find that an external magnetic field not only leads to adverse effects but can even stimulate spin dynamics. The spin mixing amplitude is not large for zero magnetic offset field, but shows a pronounced maximum for finite magnetic field values as predicted in [13,17]. The observation and understanding of this resonance in self-driven spin dynamics in quantum gases is central for detailed magnetic state manipulation. Quantum control for general spin systems (for $F = 1$ see [12]) based on this spinor resonance process might lead to new schemes for spin entanglement and quantum information applications with spinor gases.

The experimental setup has been described in [6] and the procedure resembles the one in [13]. We prepare degenerate ^{87}Rb ensembles in the $F = 2$, $m_F = -2$ state containing typically 3×10^5 atoms with a condensate fraction of ≈ 0.75 in an optical dipole trap (trapping frequencies ω_x:ω_y:$\omega_z \approx 2\pi \times 14.5$:105:600 s^{-1}). A radio frequency $\pi/2$-pulse of typically 40 μs duration rotates this state to our initial state $\zeta^{\mathrm{ini}}(0) = (1/4, 1/2, \sqrt{6}/4, 1/2, 1/4)^T$ [18]. After holding the sample for a variable time, t, at a well defined magnetic offset field, we switch off the trapping potential. The population in each spin component is extracted from absorption images after Stern-Gerlach separation during time of flight [5,6,19]. Figure 1 shows the

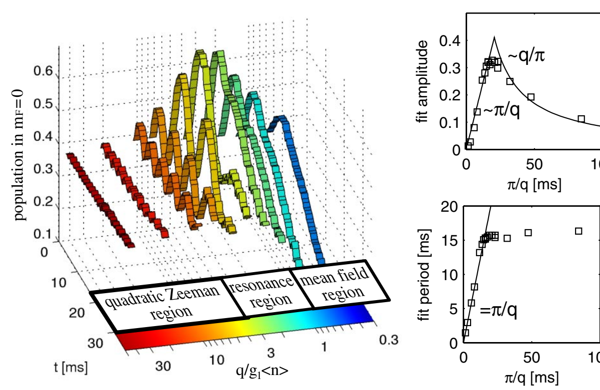

FIG. 1 (color online). Left: Temporal evolution of the $m_F =$ 0-population for different ratios of quadratic Zeeman and interaction energy (see text). Right: Magnetic field dependence of the amplitude and period of the $m_F = 0$ population as extracted from a sinusoidal fit to the oscillatory part of the data ($\langle g_1 n \rangle =$ 54 s^{-1}).

temporal evolution of the $m_F = 0$-population in dependence of the relative value of the quadratic Zeeman frequency, q, and the mean field spin mixing frequency, $g_1\langle n\rangle$. The magnetic field dependence is parameterized by $q = p^2/\omega_{\rm hfs}$ with $p = \mu_B B/2\hbar$ and the ^{87}Rb ground state hyperfine splitting $\omega_{\rm hfs} \approx 2\pi \times 6.835$ GHz. The spin-dependent mean field interaction is proportional to the density, n, of the sample and for ^{87}Rb dominated by the parameter g_1 introduced below.

Our observations show that the whole spin mixing dynamics depends critically on the relative size of the energies associated to the quadratic Zeeman shift and the spin-dependent mean field interaction. Interestingly, the oscillation amplitude in Fig. 1 is reduced whenever one of these energies dominates, i.e. in both the quadratic Zeeman regime ($q \gg g_1\langle n\rangle$) and the mean field regime ($q \ll g_1\langle n\rangle$). A maximum occurs close to balanced quadratic Zeeman and mean field contributions. The important point is, that these two effects compete with each other. The quadratic Zeeman effect lifts the energy of the $m_F = 0$ state with respect to the other states, while the mean field interaction lowers it. More precisely, the phase evolution due to these energy contributions is occurring in opposite directions. However, as spin mixing is a coherent process, this phase determines the direction of spin mixing. The accumulation of many particles in one state can thus only happen for slow phase evolution, i.e. close to the balanced case.

We want to emphasize, that although we consider only two-body interactions, the spin mixing resonance presented in this Letter crucially relies on nonlinear mean field effects like self- and cross-phase modulation, i.e. the coupling between different spin states depends on the density and phase of the individual spin components. It is therefore fundamentally different from the Rabi-like resonance observed in a two-particle system [11], which is described by a fixed coupling.

For clarity, we will start our analysis by a discussion of the qualitatively expected features in single mode approximation (SMA), i.e., neglecting a spatial variation of the spinor composition, which will be discussed later. In particular, we present and interpret analytic solutions for the asymptotic behavior in the regimes of high and low magnetic field. Our analysis is based on the spinor evolution $i\dot{\zeta} = \frac{\partial H}{\partial \zeta^*}$ due to the mean field Hamiltonian [4]:

$$H = -p\langle F_z\rangle - q\langle 4 - F_z^2\rangle + \frac{g_1\langle n\rangle}{2}\langle \vec{F}\rangle^2 + \frac{g_2\langle n\rangle}{2}|S|^2, \tag{1}$$

where $\vec{F} = (F_x, F_y, F_z)$ is the spin operator, $\langle\rangle$ denotes an expectation value, and $S = \zeta_0^2/2 - \zeta_{+1}\zeta_{-1} + \zeta_{+2}\zeta_{-2}$ is the spin-singlet amplitude.

Spin mixing occurs as a consequence of two-particle collisions and can be classified by the total spin f of the colliding pair. For $F = 2$ the allowed values are $f = 0, 2, 4$. The spin mixing interactions are parameterized by the coupling coefficients $g_1 = \frac{4\pi\hbar^2}{m}\frac{a_4 - a_2}{7}$ and $g_2 = \frac{4\pi\hbar^2}{m} \times \frac{4}{5}\frac{7a_0 - 10a_2 + 3a_4}{7}$ [4], using the spin-dependent s-wave scattering lengths a_f. The dynamics of $F = 2$ spinor condensates will in general be a complex superposition of the different mixing processes summarized in Table I (we use the notation (i) for waves/particles in the $m_F = i$ state). This table also lists the relative quadratic Zeeman energy shifts of the involved states. ^{87}Rb has the advantage that the value of g_2 is very small [20], such that the processes listed in the lower part of Table I are largely suppressed and can be neglected in the following [21]. In addition, we will concentrate on the specific initial state $\zeta^{\rm ini}(0)$ used in our experiments. For the population evolution in the limit of low magnetic field ($q \ll g_1\langle n\rangle$), i.e. the "mean field region," we find to first order:

$$\begin{aligned} |\zeta_0^{\rm mf}|^2 &= \frac{3}{8}\left(1 - \frac{q}{2g_1\langle n\rangle}[\cos(4g_1\langle n\rangle t) - 1]\right) \\ |\zeta_{\pm1}^{\rm mf}|^2 &= \frac{1}{4}\left(1 + \frac{q}{2g_1\langle n\rangle}[\cos(4g_1\langle n\rangle t) - 1]\right) \\ |\zeta_{\pm2}^{\rm mf}|^2 &= \frac{1}{16}\left(1 - \frac{q}{2g_1\langle n\rangle}[\cos(4g_1\langle n\rangle t) - 1]\right) \end{aligned} \tag{2}$$

This mean field dominated evolution is just a sinusoidal oscillation between the spin components and shows a magnetic field independent period $T_{\rm mf} = \frac{\pi}{2g_1\langle n\rangle}$ as observed in Fig. 1. Furthermore, these equations indicate that the oscillation amplitude in this regime should be proportional to the quadratic Zeeman shift q, which is reflected in Fig. 1.

In the other limit at high magnetic field, i.e. the quadratic Zeeman regime with $q \gg g_1\langle n\rangle$, the population evolution is dominated by the quadratic Zeeman energy and we find:

$$\begin{aligned} |\zeta_0^{qZ}|^2 &= \frac{3}{8}\left\{1 - \frac{g_1\langle n\rangle}{2q}\left[2(\cos(2qt) - 1) + \frac{\cos(4qt) - 1}{2}\right]\right\} \\ |\zeta_{\pm1}^{qZ}|^2 &= \frac{1}{4}\left\{1 + \frac{g_1\langle n\rangle}{2q}\left[\frac{3(\cos(2qt) - 1)}{4} - \frac{\cos(6qt) - 1}{12}\right]\right\} \\ |\zeta_{\pm2}^{qZ}|^2 &= \frac{1}{16}\left\{1 + \frac{g_1\langle n\rangle}{2q}\left[\frac{3(\cos(4qt) - 1)}{2} + 3(\cos(2qt) - 1)\right.\right. \\ &\qquad \left.\left. + \frac{\cos(6qt) - 1}{3}\right]\right\}. \end{aligned} \tag{3}$$

The oscillation amplitude in this regime decays with $\frac{1}{q}$ in accordance to the data in Fig. 1. However, now several

TABLE I. Four wave mixing processes in $F = 2$ spinor BEC.

Process	Coupling	q.Z. energy diff.
$(0) + (0) \leftrightarrow (+1) + (-1)$	g_1	$2q$
$(+1) + (+1) \leftrightarrow (+2) + (0)$	g_1	$4q$
$(-1) + (-1) \leftrightarrow (0) + (-2)$	g_1	$4q$
$(+1) + (-1) \leftrightarrow (+2) + (-2)$	g_1	$6q$
$(0) + (0) \leftrightarrow (+1) + (-1)$	g_2	$2q$
$(+1) + (-1) \leftrightarrow (+2) + (-2)$	g_2	$6q$
$(0) + (0) \leftrightarrow (+2) + (-2)$	g_2	$8q$

frequencies are involved as a result of the different mixing processes in $F = 2$ spin dynamics. The oscillation periods reflect the different quadratic Zeeman shifts for the possible g_1 mixing processes as listed in Table I. For the chosen initial state, spin mixing is dominated by the $\cos(2qt)$ term in Eq. (3) connected to the $(0) + (0) \leftrightarrow (-1) + (+1)$ process, which has a factor of 4 higher weight than the $\cos(4qt)$ term.

From the above tendencies in the population oscillation, it is clear, that a maximum amplitude must occur at an intermediate magnetic field value, i.e. the resonance found in Fig. 1.

In the following, we will develop some more qualitative physical insights by an interpretation of the resonance phenomenon in terms of ''phase matching'' in four wave mixing (see Fig. 2). First, we note that given the prefactor $\frac{1}{16}$, the oscillation amplitude of the $m_F = \pm 2$ wave is relatively small in both the mean field regime and the quadratic Zeeman regime. This justifies an approximate view as a pure $(-1) + (+1) \leftrightarrow (0) + (0)$ four wave mixing process. In contrast to nonlinear optics or four wave mixing in single component condensates [23], we do not deal with wave vector or momentum modes [24,25] but with spin modes, i.e. here the $m_F = +1$ wave and the $m_F = -1$ wave couple to 2 times the $m_F = 0$ wave (this view is justified, as we are considering trapped samples in a single momentum state). Spin mixing in trapped samples corresponds to degenerate collinear four wave mixing [25] and (in contrast to single component four wave mixing) in principle allows infinite interaction times, only limited by finite temperature effects [9,13,26–28].

In view of the optical analogy, it is obvious, that phase matching considerations are essential to understand the resonance in spinor four wave mixing. The important point is, that the value of the relative phase of the initial and final waves or spin components determines the direction of wave mixing. In our case, the (0) wave will be populated if the combined phase of the $(+1) + (-1)$ waves is ahead of twice the (0) wave phase, i.e. $\theta = \varphi_{+1} + \varphi_{-1} - 2\varphi_0 \in [0 \ldots \pi]$ and it will be depopulated if $\theta \in [\pi \ldots 2\pi]$ (modulo 2π).

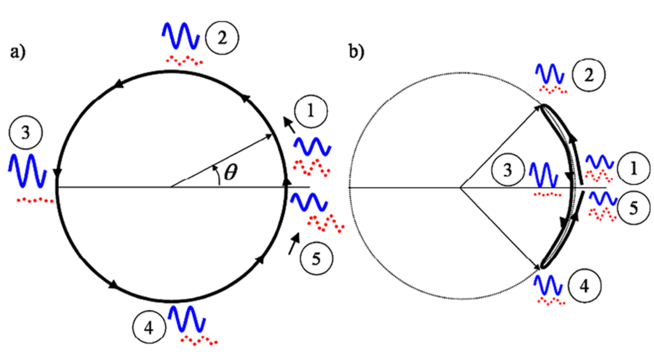

FIG. 2 (color online). Schematic representation of four wave mixing in (a) the quadratic Zeeman regime and (b) the mean field regime. In the upper part, the (0) waves (upper wave) get populated, while in the lower part, the (+1) and (−1) wave (lower wave) increase. The wave symbols show the populations and relative phase of the (0) and (+1) and (−1) waves during one oscillation cycle going from 1 to 5.

In general, the relative phase evolution of the spinor components in spin mixing is highly nontrivial, as in addition to the quadratic Zeeman energy shifts it depends on the spin coupling and the spin component populations in a nonlinear way. We find that for our system, the competition between mean field driven dephasing (tending to decrease θ) and quadratic Zeeman shift driven dephasing (tending to increase θ) determines the evolution of the system. Most importantly, the evolution depends on the relative size of the quadratic Zeeman energy shift and the maximally achievable mean field shifts, as shown in Fig. 2. For large magnetic fields, i.e. always negligible mean field energy shifts, θ will continuously grow, i.e. the (± 1) wave evolves faster than the (0) wave, and the population transfer shows an oscillatory behavior depending on which wave is lagging behind at which instant [Fig. 2(a)]. In this regime, the oscillation period is expected from Eq. (2) to be given by $\frac{\pi}{q}$. Furthermore, the oscillation amplitude, which depends on the unidirectional mixing time, should be proportional to this period. Both these expectations are confirmed by the data, as shown in the inset of Fig. 1.

For small magnetic fields, the mean field energy shift grows with increasing population in the (0) wave, until it exceeds the quadratic Zeeman shift and thus reverses the evolution of θ, i.e., the (0) wave will speed up and decrease its lag behind the (± 1) wave, eventually overtaking it. In this case, θ will remain confined in the interval $[-\pi \ldots \pi]$ and oscillate around $\theta = 0$ [Fig. 2(b)]. In this regime, the population oscillation amplitude is expected to decrease with decreasing q, i.e. at lower magnetic field, as less population transfer is necessary to create a mean field energy of the size of the quadratic Zeeman shift. This decrease in amplitude is also confirmed by the data in Fig. 1.

In the resonance region at intermediate magnetic field, the relative movement of the (0) and (± 1) waves is very slow, with θ being on the border of oscillation and continuous increase. This leads to long time unidirectional spin mixing and thus maximum amplitude.

We want to point out that also the initial direction of spin mixing increasing the (0) wave amplitude as observed in Fig. 1 can be explained by simple arguments. The chosen initial state ζ^{ini} has zero phase shift $\theta = 0$ and shows no mean field dephasing between the (± 1) and (0) waves. This is due to the fact, that it originates from the fully stretched (-2) eigenstate subjected to a 90° rotation. As the mean field part of the Hamiltonian is invariant under rotations, ζ^{ini} stays a mean field eigenstate. Consequently, the quadratic Zeeman energy shift will always cause the (± 1) wave to evolve faster than the (0) wave or in other words, θ will initially always grow. The transfer of particles going in the direction of the wave lagging behind will thus result in an initial increase of the (0) wave (see Fig. 2).

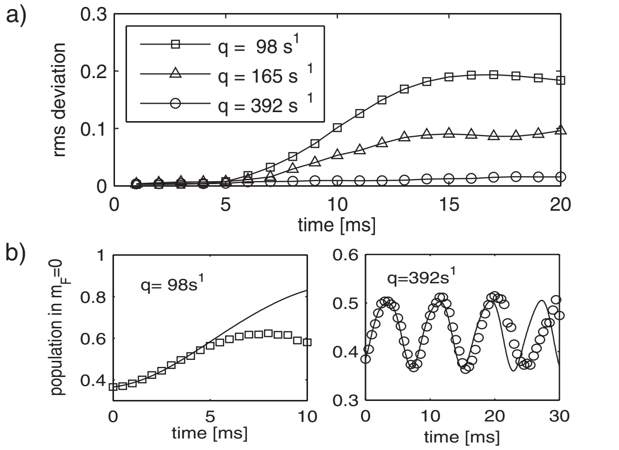

FIG. 3. (a) deviation (rms of $m_F = 0$ population) of SMA theory fit ($g_1\langle n\rangle = 54\ \mathrm{s}^{-1}$ fixed) from our data (Fig. 1). The abscissa specifies the time range over which the fit was performed. (b) two examples of fits compared to data.

In addition to the qualitative understanding of the tendencies observed in Fig. 1 within the SMA, a quantitative comparison allows us to deduce the validity limits of this approximation. Although the initial state is prepared in a single spatial mode, its size in the weak trap direction of $\approx 100\ \mu$m is much larger than the g_1-spin healing length $\xi_s = \hbar/\sqrt{2g_1 nm} \approx 2.6\ \mu$m. Similar to the simulations in [28] and the experiment in [10], we thus expect spatial structures to form after some time due to local differences in spin dynamics. Indeed, we observe the breakdown of the SMA, indicated by a strong damping of the oscillation of the (spatially averaged) populations at low q. However, for high q, the spinor oscillations last significantly longer. This can be understood as the mean field spinor evolution is characterized by a density dependent coupling constant $g_1\langle n\rangle$, while in the quadratic Zeeman regime, it is determined by q. For mean field driven spin dynamics, the higher density parts of the spinor condensate will thus dephase relative to the lower density parts, and population oscillations in the total fractions will be washed out.

In Fig. 3(a), we study the rms deviation of the measured spinor evolution from best-fit theoretical curves based on the SMA as a function of evolution time. In the mean field regime, the SMA breaks down after ≈ 5 ms (squares), while there is a near perfect agreement over more than 20 ms in the quadratic Zeeman region (circles). This behavior is also reflected in the corresponding time sequences and fit curves shown in Fig. 3(b). Our most important observation in this respect is that even for condensate sizes much above the spin healing length, the single mode approximation works remarkably well once the quadratic Zeeman effect dominates the relative phase evolution.

In conclusion, we have investigated a magnetically tunable resonance in coherent spin dynamics and have analyzed this phenomenon in terms of phase matching considerations, which are applicable to general values of total spin. In the future, this resonance will allow the controlled use of spin dynamics to fully convert one spinor state into another, even with local control, by shifting in and out of the validity range of the single mode approximation. These possibilities open new perspectives for spatiotemporal tailoring of the spinor condensate wave function, e.g. for the creation of highly nonclassical spin states with spatially varying degree of entanglement.

We acknowledge funding by the Deutsche Forschungsgemeinschaft within No. SPP 1116. P. N. acknowledges support from the German AvH foundation and from the KULeuven Research Council.

[1] T.-L. Ho, Phys. Rev. Lett. **81**, 742 (1998).
[2] T. Ohmi and K. Machida, J. Phys. Soc. Jpn. **67**, 1822 (1998).
[3] C. K. Law, H. Pu, and N. P. Bigelow, Phys. Rev. Lett. **81**, 5257 (1998).
[4] M. Koashi and M. Ueda, Phys. Rev. Lett. **84**, 1066 (2000).
[5] J. Stenger *et al.*, Nature (London) **396**, 345 (1998).
[6] H. Schmaljohann *et al.*, Phys. Rev. Lett. **92**, 040402 (2004).
[7] M.-S. Chang *et al.*, Phys. Rev. Lett. **92**, 140403 (2004).
[8] T. Kuwamoto *et al.*, Phys. Rev. A **69**, 063604 (2004).
[9] H. Schmaljohann *et al.*, Appl. Phys. B **79**, 1001 (2004).
[10] J. M. Higbie *et al.*, Phys. Rev. Lett. **95**, 050401 (2005).
[11] A. Widera *et al.*, Phys. Rev. Lett. **95**, 190405 (2005).
[12] M.-S. Chang *et al.*, Nature Phys. **1**, 111 (2005).
[13] J. Kronjäger *et al.*, Phys. Rev. A **72**, 063619 (2005).
[14] L. E. Sadler *et al.*, cond-mat/0605351.
[15] H. Pu, S. Raghavan, and N. P. Bigelow, Phys. Rev. A **61**, 023602 (2000).
[16] D. R. Romano and E. J. V. de Passos, Phys. Rev. A **70**, 043614 (2004).
[17] W. Zhang *et al.*, Phys. Rev. A **72**, 013602 (2005).
[18] We use the notation $\psi = \sqrt{n}[\zeta_{+2}, \zeta_{+1}, \zeta_0, \zeta_{-1}, \zeta_{-2}(t)]^{\mathrm{T}}$ for the vector order parameter of the spinor condensate.
[19] The magnetic offset field has a 2 mG uncertainty and a shot-to-shot stability of 300 μG as measured with rf spectroscopy. The shot-to-shot density fluctuations are below 3%, ensuring reproducible experimental conditions.
[20] A. Widera *et al.*, cond-mat/0604038.
[21] We checked the validity of this assumption by confirming that the initial state $\zeta^{(0)}(0) = (\sqrt{6}/4, 0, -1/2, 0, \sqrt{6}/4)^T$ shows no visible spin mixing within the first 15 ms, which is the relevant timescale for coherent evolution in our experiment [13]. This initial state evolves solely due to the g_2 coupling: $(0) + (0) \leftrightarrow (+2) + (-2)$ [22].
[22] H. Saito and M. Ueda, Phys. Rev. A **72**, 053628 (2005).
[23] L. Deng *et al.*, Nature (London) **398**, 218 (1999).
[24] J. P. Burke *et al.*, Phys. Rev. A **70**, 033606 (2004).
[25] E. V. Goldstein and P. Meystre, Phys. Rev. A **59**, 3896 (1999).
[26] H. J. Lewandowski *et al.*, Phys. Rev. Lett. **91**, 240404 (2003).
[27] M. Erhard *et al.*, Phys. Rev. A **70**, 031602 (2004).
[28] J. Mur-Petit *et al.*, Phys. Rev. A **73**, 013629 (2006).